WNT5A Is a Regulator of Fibroblast Proliferation and Resistance to Apoptosis

Louis J. Vuga[1], Ahmi Ben-Yehudah[2], Elizabetha Kovkarova-Naumovski[1], Timothy Oriss[1], Kevin F. Gibson[1], Carol Feghali-Bostwick[1], and Naftali Kaminski[1]

[1]Dorothy P. and Richard P. Simmons Center for Interstitial Lung Diseases, Division of Pulmonary, Allergy, and Critical Care Medicine, and [2]Pittsburgh Development Center, Magee-Women's Research Institute and Foundation, University of Pittsburgh School of Medicine, Pittsburgh, Pennsylvania

Usual interstitial pneumonia (UIP) is a specific histopathologic pattern of interstitial lung fibrosis that may be idiopathic or secondary to autoimmune diseases and environmental exposures. In this study, we compared gene expression patterns in primary fibroblasts isolated from lung tissues with UIP histology and fibroblasts isolated from lung tissues with normal histology using expression microarrays. We found that WNT5A was significantly increased in fibroblasts obtained from UIP lung tissues compared with normal lung fibroblasts, an observation verified by quantitative real-time RT-PCR and Western blot. Because the role of WNT5A in UIP is unknown, we treated normal lung fibroblasts or UIP lung fibroblasts with WNT5A, and found that WNT5A increased proliferation as well as relative resistance to H_2O_2-induced apoptosis. This effect was not mediated through the canonical WNT/β-catenin pathway, as WNT5A induced a decrease in β-catenin levels in the same cells. In addition, WNT5A induced increases in fibronectin and α_5-integrin in normal lung fibroblasts. Collectively, our data suggest that WNT5A may play a role in fibroblast expansion and survival characteristics of idiopathic pulmonary fibrosis and other fibrotic interstitial lung diseases that exhibit UIP histological patterns.

Keywords: gene expression; idiopathic pulmonary fibrosis; cell growth; apoptosis; extracellular matrix

Usual interstitial pneumonia (UIP) is a specific histological pattern of lung scarring that can be secondary to environmental exposures, autoimmune disease, or when the etiology is unknown, the hallmark of idiopathic pulmonary fibrosis (IPF). IPF is the best-studied form of UIP, and is associated with the poorest prognosis among diseases with UIP lung histology (1–4).

It has been recently proposed that UIP histology is likely the result of an abnormal response of alveolar epithelial cells to injury (5). This epithelial response leads to migration, proliferation, and activation of fibroblasts, with the formation of active fibroblastic/myofibroblastic foci, a pathologic hallmark of the disease (2, 6). Exaggerated accumulation of fibroblasts, extracellular matrix deposition, and irreversible destruction of the lung parenchyma determine the lung phenotype in UIP (7–12). Therefore, understanding the behavior of fibroblasts is critical in comprehending the pathogenesis of pulmonary fibrosis.

Several studies have addressed differences between lung fibroblasts isolated from fibrotic lungs and control lungs. Fibroblasts from early pulmonary fibrosis exhibit higher proliferation rates (13), increased secretion of extracellular matrix proteins, including fibronectin and insulin growth factor binding protein 3 and 5, and exaggerated migratory response to CCL21 (14–16). In contrast, normal lung fibroblasts secrete more collagenase (17). Recent reports suggest that fibroblasts transform into myofibroblasts in fibrotic lungs, with significant differences in their molecular characteristics and localized activities (18–22). Although several studies have analyzed whole-lung gene expression patterns in IPF and control lungs (23–27) and identified multiple differentially expressed genes, only one study compared fibrotic lung fibroblasts to normal lungs fibroblasts using microarrays, and the authors did not find any global differences in their response to transforming growth factor-β1 (28).

In this study, we compared gene expression patterns in primary human lung fibroblasts isolated from lung tissues of explants with UIP histology and normal lung tissues of organ donors using expression microarrays. Although we did not identify statistically significant global changes, we identified WNT5A as one of the few genes that were overexpressed in fibroblasts obtained from UIP lung tissues. We verified the microarray results and explored the potential effects of WNT5A in normal lung fibroblasts with respect to fibrosis-relevant behaviors.

Portions of these findings have been presented at the American Thoracic Society conference in San Diego, May 2006.

CLINICAL RELEVANCE

Our results suggest a mechanism by which enhanced WNT5A secretion may promote fibroblast proliferation and survival in usual interstitial pneumonia (UIP) lungs, despite the presence of multiple proapoptotic signals, and thus suggest a novel explanation for the "apoptosis paradox." They also highlight a potential role for the noncanonical WNT pathway in determining the lung phenotype in UIP.

MATERIALS AND METHODS

Materials

For microarrays, we used Codelink Human Uniset I (Amersham Bioscience, Piscataway, NJ). Real-time PCR reagents and primers were obtained from Applied Biosystems (ABI, Foster City, CA). We purchased the following chemicals and reagents: Celltiter96 Aqueous One solution reagent (Promega, Madison, WI); propidium iodide, anti–α5-integrin and anti-fibronectin (Chemicon International, Temecula, CA); anti–β-catenin and anti–glycogen synthase kinase (GSK) 3β (Santa Cruz Biotechnology, Santa Cruz, CA); anti–β-actin (Sigma, St. Louis, MO); Phospho-β-catenin (Cell Signaling, Beverly, MA); and chemiluminescence (PerkinElmer Life Sciences, Boston, MA). Mouse recombinant WNT5A was obtained from R&D Systems Inc. (Minneapolis, MN). Parent mouse fibroblasts CRL-2648 and WNT5A transfected mouse

(*Received in original form June 1, 2008 and in final form December 17, 2008*)

This work was supported in part by National Institutes of Health grant HL 073745 (L.J.V., C.F.-B., K.F.G., and N.K.), and by the Dorothy P. and Richard P. Simmons chair for Pulmonary Research.

Correspondence and requests for reprints should be addressed to Naftali Kaminski, M.D., University of Pittsburgh, School of Medicine, 3459 Fifth Ave., 628NW Montifore, Pittsburgh, PA 15213. E-mail: kaminskin@upmc.edu

Am J Respir Cell Mol Biol Vol 41. pp 583–589, 2009
Originally Published in Press as DOI: 10.1165/rcmb.2008-0201OC on February 27, 2009
Internet address: www.atsjournals.org

fibroblasts (CRL-2814) were obtained from the American Type Culture Collection (Manassas, VA). Active caspase-3 ELISA kit was obtained from Calbiochem (San Diego, CA).

Cell Culture

Normal lung fibroblasts were acquired from lung tissue of organ donors at the University of Pittsburgh Medical Center (Pittsburgh, PA). The experimental protocol was approved by the University of Pittsburgh Institutional Reviews Board. Early passages (4–7) of cells were cultured in a humidified atmosphere containing 5% of CO_2 in Dulbecco's modified Eagle's medium (Cellgro, Herndon, VA), supplemented with 10% FBS (American Type Culture Collection), 1% penicillin (Cellgro), and maintained in a humidified incubator (Kendro Lab, New Town, CT) at 37°C. All cells were grown on cell culture plates (Corning-Costar Corp., Corning, NY) until 70 to 80% confluence.

WNT5A-transfected mouse fibroblasts and the parent mouse fibroblasts were maintained according to the manufacturer's protocol. The supernatant was collected and stored at −80°C until use. Supernatant of parental cell line CRL-2648 served as a control for WNT5A containing supernatant of fibroblast line CRL-2814. WNT5A content of both supernatants was routinely checked by Western blotting.

Total RNA Extraction

Total RNA was extracted from lung fibroblasts using TRIzol reagent (GIBCO-BRL, Gaithersburg, MD) according to the manufacturer's protocol. The quantity of the RNA was determined by using a Nanodrop (Nanodrop 3.0.0) spectrophotometer, and its quality was measured using an Agilent Bioanalyzer 2,100 (both from Agilent Technologies, Wilmington, DE). Total RNA was stored at −80°C until use.

Microarray Analysis

Total RNA was extracted from three normal lung fibroblasts (donors 5, 6, and 7) and four fibroblasts from lung tissues with UIP histology (patients 19, 20, 21, and 22). The total RNA was then used as a template to generate double-stranded cDNA and biotin-labeled cRNA, as recommended by the manufacturer of the arrays and as previously described (23). Fragmented cRNA was hybridized to Codelink Uniset I slides. After hybridization, arrays were washed and stained with streptavidin-AlexaFluor 647. The arrays were scanned using a Genepix 4000B microarray scanner. Images were analyzed using Codelink expression II analysis suite, and visually inspected for defects and quality control parameters as recommended by the manufacturer. Data files were imported into a microarray database, linked with updated gene annotations using SOURCE (available at: http://genome-www5.stanford.edu/cgi-bin/SMD/source/sourceSearch), and median scaled. Based on our previous experience (23), all expression levels below 0.01 were brought to 0.01. Only transcripts with Entrez Gene IDs were included in analysis. Statistical analysis was performed using the ScoreGenes gene expression package (http://www.cs.huji.ac.il/labs/compbio/scoregenes), and data visualization was performed using Genomica (http://genomica.weizmann.ac.il/) and Spotfire Decision Site 8.0 (Spotfire, Göteborg, Sweden) (29). The complete set of gene array data has been deposited in the Gene Expression Omnibus database with GEO serial accession number GSE10921 (http://www.ncbi.nlm.nih.gov/geo) according to minimal information about microarray experiments (MIAME) guidelines. The general approach to analysis has been previously described by us (30). Correction for multiple testing was performed by calculating the false discovery rate, as previously described (30). Genes were defined as being substantially changed if they had a threshold number of misclassifications (TNoM) score of 0 and a *t* test with a *P* value of less than 0.05, as previously described (31).

Quantitative Real-Time PCR

Five fibroblast lines from lung tissue with UIP histology and five normal lung fibroblast lines were cultured, and total RNA was extracted as described previously here. All reagents and analysis software used for quantitative RT-PCR (qRT-PCR) experiment were obtained from Applied Biosystems (ABI, Foster City, CA). The Taqman Gold kit (catalog no. 430-4441) was used for measuring mRNA of WNT5A according to the manufacturer's protocol. Primers of WNT5A (catalog no. Hs00263977_ml), human β-glucuronidase (catalog no. Hs99999908_m1), as well as prism 96-well optical reaction plates (no. 430,673) were obtained from ABI. cDNA was added to each reverse-transcribed well, and mRNA was measured using an ABI prism 7900HT, followed by the application of SDS 2.2.2 analysis software (Applied Biosystems) for statistical analysis.

Cell Proliferation Assays

Normal lung fibroblasts were placed in 96 well plates, 5,000 cells in 100 μL medium per well. Cells were treated with 3μg/ml of recombinant WNT5A, incubated at 37°C for 72 hours in a humidified atmosphere containing 5% of CO_2. Cells proliferation was measured using CellTiter Aqueous One solution reagent protocol (Promega). The assay was read at 490 nm using Softmaxpro (Molecular Devices Corp., Sunnyvale, CA). 4 control and 3 UIP fibroblast lines were used for proliferation studies. Assays were repeated 3 times.

Apoptosis

Normal lung fibroblasts (three primary lung fibroblast lines) were cultured as described previously here, serum starved for 24 hours, and stimulated with 3 μg/ml WNT5A for 24 hours. Apoptosis was equally induced in cells stimulated with and without WNT5A using 1 mM H_2O_2 for 20 hours. Cells were trypsinized, collected, and resuspended in 1% paraformaldehyde in PBS (Cambrex, Walkersville, MD) (pH 7.4; 1–2 × 10^6 cells/ml), and placed on ice for 60 minutes. Cells were stained according to the APO-DIRECT protocol (Chemicon International Inc.) for detecting apoptosis. After 30-minute incubation in the dark at room temperature, the assay was measured by flow cytometry and analyzed using Cellquest software (Becton Dickinson, Mansfield, MA). For caspase-3 determinations, cell samples were extracted using the extraction protocol of the active caspase-3 ELISA kit (Calbiochem). Samples were analyzed according to the manufacturer's protocol and using Deltasoft 111 version 2.243 (Bio-Rad, Hercules, CA).

WNT5A Inhibition

Cells (1.5 × 10^5) were seeded in six-well plates and transfected with short interfering RNA (siRNA) (hWNT5A) (Dharmacon, Lafayette, CO) or control siRNA. siRNA (hWNT5A, 4 ng) was mixed in 250 μl optimem (Invitrogen, Carlsbad, CA) for 5 minutes and followed by incubating in a mixture of 10 μl liptofectamine 2,000 (Invitrogen) and 250 μl optimem for 20 minutes and added to each well. Apoptosis induction was performed 48 hours after transfection, as we observed significant down-regulation of WNT5A at this time point and 72 hours after transfection by RT-PCR and Western blotting.

Protein Extraction

Normal lung fibroblasts were cultured as described previously here (*see* CELL CULTURE section), serum starved, and treated for 24 hours with 1, 2, or 3 μg/ml recombinant WNT5A (R&D Systems). The Cells were washed three times with PBS, lysed in 1 ml lysis buffer (50 mM Tris HCl [pH 7.5], 500 mM NaCl, NP-40, 0.25% nadeoxycholate, 20 mM NaF), and supplemented with 1 μl/ml protease inhibitor cocktail II (Sigma). The lysates were placed on a slow shaker at 4°C for 20 minutes, centrifuged at 12,000 × *g* for 15 minutes, and stored at −80°C. Concentrations of the proteins in the lysates were determined by Bicinchoninic acid protein assay with BSA as standard (Pierce, Rockford, IL).

Western Blots

Cells were cultured as described previously here, serum starved for 24 hours, and treated for 24 hours with 1, 2, or 3 μg/ml recombinant WNT5A (R&D Systems). The protein in the supernatant and cell lysates was measured using the Bicinchoninic acid Protein Quantitation Assay kit (Pierce), and were resuspended in lamellae buffer (R&D Systems) containing 5% β-mercaptoethanol (Sigma). The proteins were then equally loaded in wells of 8 and 10% SDS-PAGE (Bio-Rad) for high molecular weight and middle molecular weight protein, respectively. The gels were run using Mini-Protean electrophoresis module assembly (Bio-Rad) at 150 mV at 4°C in running buffer (25 mM Tris base, 192 mM glycine, and 0.1% SDS [Sigma]) in double-distilled water. This was followed by wet transfer to polyvinylidene difluoride membranes (Millipore, Bedford, MA) for 90 minutes using the Mini Trans-Blot electrophoresis transfer cell (Bio-Rad) at 280 mA

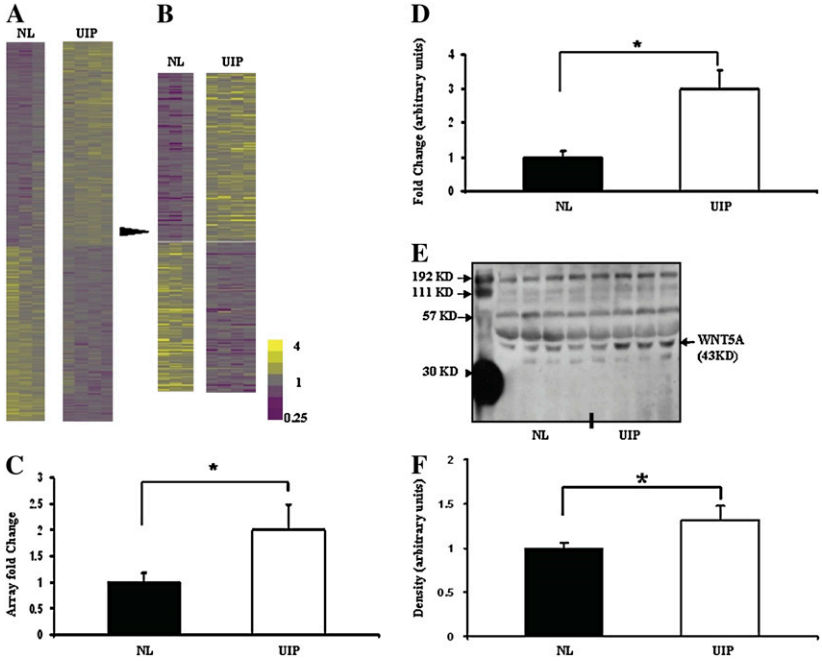

Figure 1. WNT5A is overexpressed in usual interstitial pneumonia (UIP) lung fibroblasts. (*A*) Heat map of 8,396 genes that had an Entrez Gene ID demonstrated differences in gene expression patterns between UIP lung fibroblast lines ($n = 4$) and normal lung (NL) fibroblast lines ($n = 3$). (*B*) A total of 350 genes substantially changed (TNoM = 0 and *t* test, $P < 0.05$). Up-regulated genes are presented in *yellow*, down-regulated genes in *purple*, and unchanged genes in *gray*. (*C*) WNT5A expression levels in microarray data. WNT5A gene expression was increased in UIP compared with NL (TNoM = 0, *t* test, $P < 0.05$). (*D*) Quantitative RT-PCR (qRT-PCR) verification of microarray data demonstrate increased WNT5A in UIP ($n = 5$) compared with NL ($n = 5$) ($P < 0.05$). (*E*) WNT5A protein levels were higher in UIP ($n = 4$) than NL ($n = 4$), as measured by Western blot analysis of cell supernatant. The loading control is the band at 192 kD. (*F*) Densitometric quantification of WNT5A protein levels measured by Western analysis in *E*. WNT5A was significantly higher in UIP than NL (*$P <$ 0.05). All fibroblast lines were used at early passages (4–7).

in transfer buffer (25 mM Tris [pH 7.5], 192 mM glycine, 20% methanol, and 0.025% SDS [Sigma]). The membranes were then blocked for 45 minutes with 3% BSA in Tris-buffered saline/Tween 20 (Sigma), and incubated overnight with the following primary antibodies: β-catenin, GSK-3α/β (Santa Cruz Biotechnology); WNT5A (R&D Systems); phospho-β-catenin (serine 45/threonine 41), phospho-β-catenin (serine 33/37/threonine 41) (Cell Signaling); fibronectin (Chemicon International); and β-actin (Sigma). Membranes were washed three times for 15 minutes each before and after they were incubated with appropriate secondary antibody. β-Actin was used as a loading control, except for supernatants where nonspecific bands were used as loading controls. The washed membranes were exposed to chemiluminescent substrate (PerkinElmer Life Sciences), and then visualized using autoradiography (Kodak, Pittsburgh, PA). To strip the antibodies, membranes were incubated in slow shaking stripping buffer (1 mM HCl [pH 2.2]) for 45 minutes. The autoradiographs were scanned and processed using Adobe Photoshop CS2 software (Adobe Systems, San Jose, CA). Densitometry was performed using the shareware, ImageJ (http://rsbweb.nih.gov/ij/).

Immunofluorescence

Normal primary lung fibroblasts were cultured on Lab-Tek chamber slides (Nunc, Rochester, NY), serum starved for 24 hours, and stimulated with 3 μg/ml WNT5A for 24 hours. Cells were washed with PBS three times for 5 minutes each, and fixed in 2% paraformaldehyde (Sigma) for 45 minutes. Permeabilization of cells was performed by using 0.1% Triton X in PBS for 45 minutes, followed by three washes for 5 minutes with 0.5% BSA in PBS. Cells in chamber slides were blocked with 5% donkey serum (Sigma) and in 0.5% BSA in PBS for 45 minutes. Slides were incubated with anti–β-catenin (BD Bioscience, San Jose, CA) in blocking solution overnight at 4°C, followed by five washes with 0.5% BSA in PBS for 5 minutes each, and incubated with rabbit anti-mouse conjugated to Alexia 488 (Invitrogen) for 1 hour at 37°C. After staining, chamber slides were washed with 0.5% BSA in PBS five times each for 5 minutes, followed by five washes with PBS for 5 minutes each. The chambers were removed and the cover slips were immediately mounted using the mounting medium (Vector Laboratories, Burlingame, CA) containing 4′,6′-diamidino-2-phenylindole for nuclei visualization. The slides were dried overnight in the dark at 4°C, and were examined using a Leica TCS-SP2 laser scanning confocal microscope (Leica, Mannheim, Germany) equipped with appropriate lasers for simultaneous imaging of up to four fluorophores. Digital data were archived to compact disk or digital video disc, and prepared for publication using Adobe Photoshop software (Adobe Systems, Mountain View, CA).

RESULTS

WNT5A Gene Expression in Lung Fibroblasts

We observed a modest difference in gene expression pattern between normal lung fibroblasts and fibroblasts obtained from lung tissue with UIP histology (Figure 1A). Although no gene passed the false discovery rate of less than 5% correction for multiple testing, the genes that were substantially changed ($n = 350$; TNoM = 0; *t* test *P* value < 0.05) did exhibit different gene expression patterns (Figure 1B). We were particularly interested in WNT proteins in view of their known role in cell differentiation and invasion. WNT5A was significantly up-regulated in UIP lung fibroblasts (Figure 1C). We validated the array results by qRT-PCR, and determined that WNT5A mRNA was significantly up-regulated in UIP lung fibroblasts compared with normal lung fibroblasts (Figure 1D). Western blot analysis of supernatants from four UIP and four normal lung fibroblast lines confirmed a similarly significant increase in WNT5A protein (Figures 1E and 1F).

Effects of WNT5A on Lung Fibroblasts

In view of the differences in WNT5A expression in normal and UIP lung fibroblasts, we further investigated the effects of WNT5A on fibroblast proliferation, apoptosis, and extracellular matrix secretion.

To examine whether WNT5A had an effect on fibroblast proliferation, we treated normal and UIP lung fibroblasts with WNT5A for 72 hours and measured cell proliferation using the CellTiter Aqueous One solution reagent. Both normal lung fibroblast lines ($n = 4$; Figure 2A) and UIP lung fibroblast lines ($n = 3$; Figure 2B) exhibited a dose-dependent increase in proliferation in response to WNT5A treatment.

It has been shown that fibroblasts in UIP lungs transform into myofibroblasts that are resistant to apoptosis (32, 33). To examine whether WNT5A had an effect on the apoptotic response of fibroblasts, we treated normal lung fibroblasts with H_2O_2, with or without WNT5A pretreatment. A 1 mM H_2O_2 treatment of normal lung fibroblasts caused a significant increase in apoptotic cells (50.47%) compared with control cells (10.81%) (Figure 3A). Pretreatment with WNT5A reduced the number of apoptotic cells (13.50%) to near control levels (Figure 3B).

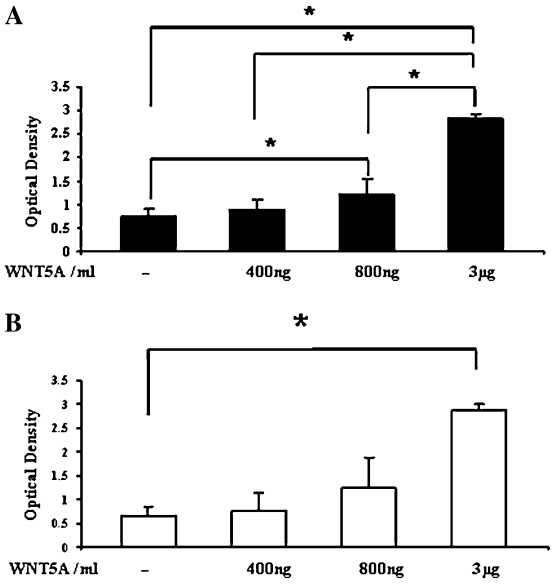

Figure 2. WNT5A promotes fibroblasts proliferation. (*A*) NL fibroblasts (*solid bars*; $n = 4$) and (*B*) UIP lung fibroblasts (*open bars*; $n = 3$) were treated with 400 ng/ml, 800 ng/ml, or 3 μg/ml of WNT5A, cultured for 72 hours, and optical densities, as a measure of cell proliferations, were significantly increased in a dose-dependant manner ($*P < 0.05$). Note that UIP lung fibroblasts were less responsive to WNT5A when compared with control (P values < 0.05). The figures shown are representatives of three experiments.

Figure 3C shows the means of apoptotic cells in sub-G1 fractions based on three experimental replicates in three normal lung fibroblast lines for the various treatment combinations.

We also determined the effect of inhibition of WNT5A on active caspase-3 levels in response to H_2O_2 in three normal and three UIP lung fibroblast lines using the active caspase-3 ELISA kit. Inhibition of WNT5A expression using siRNA (hWNT5A) caused an additional increase in active caspase-3 levels after treatment with 1 mM H_2O_2 compared with cells that had intact WNT5A levels (Figure 3E). Interestingly, the fold inductions of caspase-3 for normal and UIP fibroblasts were very similar (1.81 and 1.53, respectively), although, as expected, the total levels of active caspase-3 observed in UIP fibroblasts were significantly lower compared with normal lung fibroblasts.

To understand the effect of WNT5A on extracellular matrix, we treated normal lung fibroblasts with WNT5A and examined the levels of fibronectin and α5-integrin by Western blot. WNT5A treatment induced a significant increase in fibronectin (Figures 4A and 4B) and α5-integrin (Figure 4C) in treated cells compared with control cells. WNT5A had no effect on α-smooth muscles actin levels in human cells (data not shown).

Regulation of β-Catenin by WNT5A

To determine whether the effect of WNT5A on normal lung fibroblast proliferation and survival was induced by β-catenin, we evaluated the effect of WNT5A on β-catenin levels. Treatment of cells with recombinant WNT5A induced a dose-dependent decrease in β-catenin in normal lung fibroblasts (Figure 5A), UIP lung fibroblasts (Figure 5B), and in a lung adenocarcinoma cell line (A549 cells) (Figure 5C). A similar decrease was observed when cells were treated with WNT5A-rich conditioned media from WNT5A-transfected mouse lung fibroblasts (Figure 5D). This decrease in β-catenin levels after WNT5A treatment was also visually confirmed by immunofluorescence and confocal microscopy (Figures 5E–5J).

We investigated whether the effect of WNT5A on β-catenin levels was through the WNT/β-catenin canonical pathway, and found that WNT5A did not have an effect on GSK3β levels or its phosphorylation (Figures 5K and 5L). Similarly, WNT5A did not induce a change in phosphorylation of β-catenin at the serine 33, serine 37, or the threonine 41 positions (Figure 5M), but did induce an increase in the phosphorylation of phosphor-β-catenin at the serine 45 and threonine 41 positions (Figure

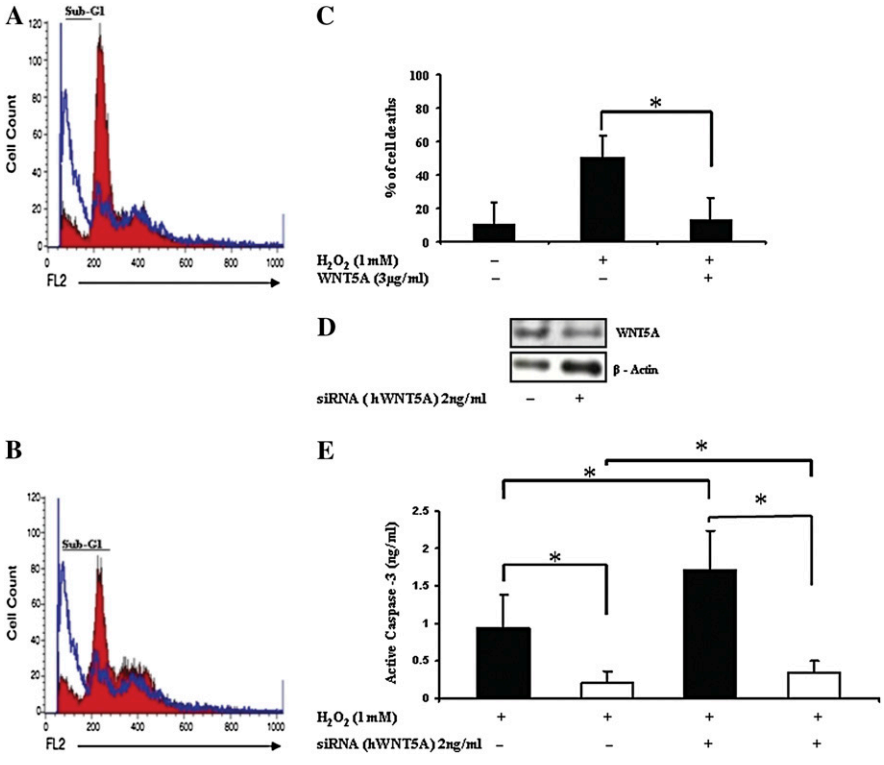

Figure 3. WNT5A inhibits H_2O_2-induced apoptosis. NL fibroblast lines ($n = 3$) were pretreated with WNT5A or vehicle control for 4 hours before H_2O_2 treatment. (*A*) Comparison of apoptosis as determined by cell count in the sub-G1 fraction between control (*red*) and 1 mM H_2O_2-treated cells (*blue*). Cells treated with 1 mM H_2O_2 showed more apoptotic cells in the sub-G1 fraction than control cells. (*B*) Comparison between combined treatments. Pretreatment of cells with WNT5A before the addition of 1 mM H_2O_2 (*red*) reduced the number of apoptotic cells compared with 1 mM H_2O_2-treated cells (*blue*). (*C*) Means of apoptotic cells in the sub-G1 fractions of three experiments expressed by a *bar* for each treatment condition. WNT5A pretreatment inhibited H_2O_2-induced fibroblast apoptosis ($*P < 0.05$). (*D*) Transfection of NL fibroblasts with WNT5A siRNA (hWNT5A) decreases protein expression of WNT5A 72 hours after transfection. (*E*) Silencing WNT5A using siRNA (hWNT5A) induced active caspase-3 in NL fibroblast lines (*solid bars*; $n = 3$) and UIP lung fibroblast lines (*open bars*; $n = 3$). The concentration of active caspase-3 was significantly increased ($*P < 0.05$) in cells treated with both 1 mM H_2O_2 and 2 ng/ml siRNA (hWNT5A) compared with control cells (scrambled siRNA) treated with H_2O_2. Active caspase-3 levels were lower in UIP fibroblasts compared with control cells.

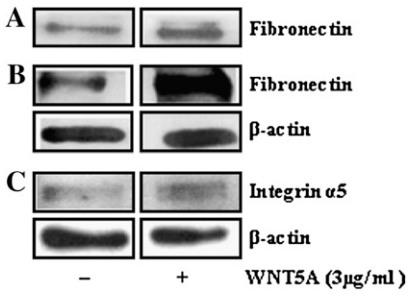

Figure 4. WNT5A effects on protein expression. (*A–C*) NL fibroblast lines treated with 3 μg/ml WNT5A showed an increase in fibronectin levels both in supernatant (*A*) and lysates (*B*). (*C*) WNT5A-treated NL showed higher level of α_5-integrin than untreated NL. β-Actin was used as a loading control.

5N), indicating that the effect of WNT5A was not mediated through the canonical WNT/β-catenin pathway.

DISCUSSION

Using gene expression microarrays, we found that the gene expression levels of WNT5A were higher in UIP lung fibroblasts compared with normal lung fibroblasts. We verified these observations, and then explored the effects of WNT5A on normal and UIP lung fibroblasts. We discovered that WNT5A was a key regulator of fibroblast proliferation and resistance to apoptosis. Treatment of fibroblasts with WNT5A induced fibroblast proliferation and resistance to H_2O_2-induced apoptosis, and WNT5A inhibition caused up-regulation of caspase-3. WNT5A also caused increases in fibronectin and in α5-integrin. Interestingly, the effects of WNT5A on fibroblast proliferation and survival were not mediated through the canonical WNT/β-catenin pathway. In fact, WNT5A treatment caused decreases in β-catenin levels, without any effect on GSK3α/β, suggesting a role for the noncanonical WNT/β-catenin pathway in regulation of fibroblast proliferation and resistance to apoptosis.

Our findings that WNT5A is secreted by UIP lung fibroblasts, and that it is protective of H_2O_2-induced apoptosis in normal lung fibroblasts, are highly relevant to the new "apoptosis paradox" paradigm recently formulated by Thannickal and colleagues (34). This paradigm suggests that the histology of UIP is characterized by two seemingly contrasting tendencies: increased apoptosis in epithelial cells, and decreased apoptosis in fibroblasts. Recently, it has been suggested that

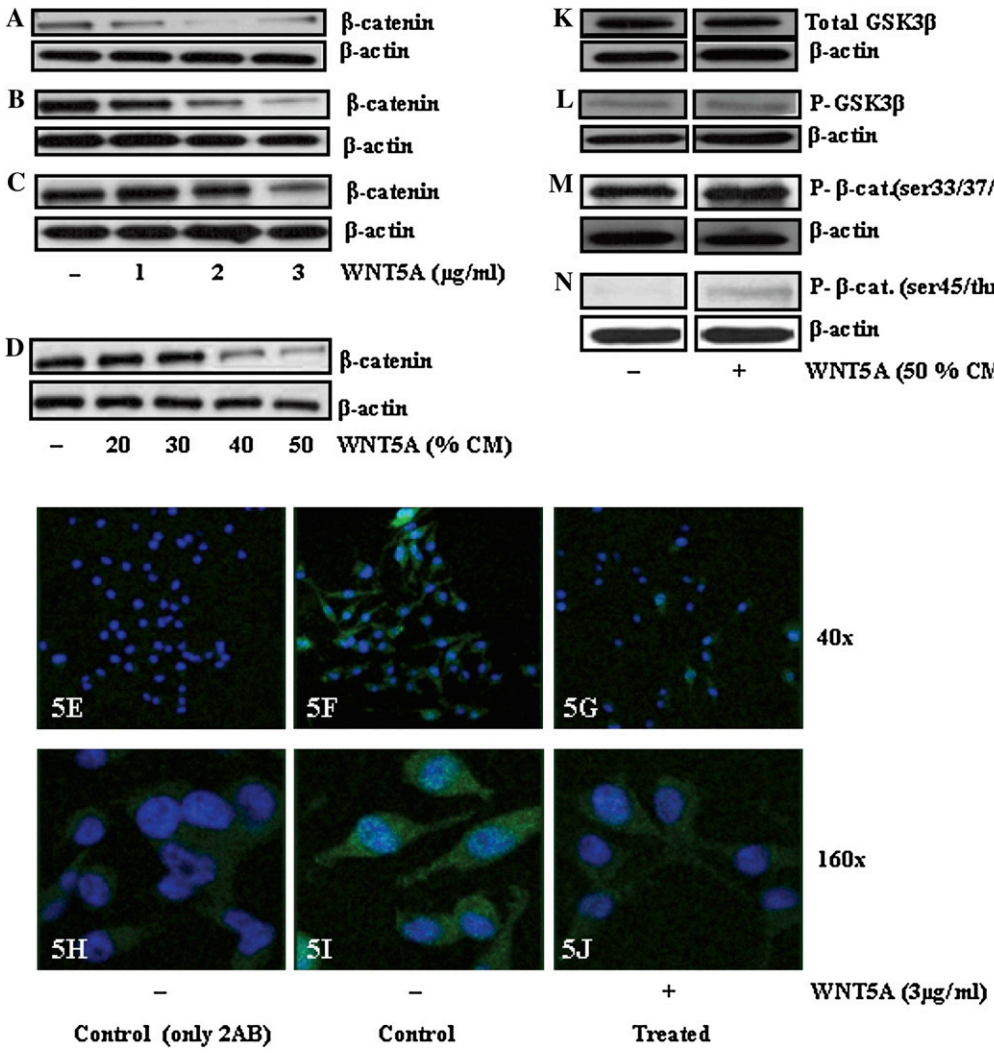

Figure 5. WNT5A decreases β-catenin levels. (*A*) NL fibroblasts, (*B*) UIP lung fibroblasts, and (*C*) A549 cells treated with 1, 2, or 3 μg/ml WNT5A showed a dose-dependent reduction of β-catenin protein level. (*D*) Treatment of NL with conditioned media (CM) containing WNT5A. Using Western blot analysis, a decreased level of β-catenin was observed (*upper panel*) and equal loading of protein was verified by applying anti–β-actin (*lower panel*). (*E–J*) Level of β-catenin visualized using immunofluorescence microscope. Cells were stained with anti–β-catenin (*green*) and DNA counterstaining, blue. Although a *bright green* staining can be observed in control cells (*F* and *I*), this staining intensity is reduced after treatment with 3 μg/ml WNT5A (*G* and *J*), similar to the background staining of negative control cells (*E* and *H*). (*K–L*) WNT signaling in lung fibroblasts. WNT5A (Supernatant) showed no effect on total GSK3β levels and P- GSK3β (ser9) levels, and no change in P–β-catenin (ser33/37/thr41) level in treated NL (*K–M*). (*N*) The protein level of phospho–β-catenin (ser45/thr41) showed an increase in WNT5A-treated NL compared with control cells. Anti–β-actin served as standard control for equal loading of each protein. All images were cut from the same individual gels.

reactive oxygen species play a significant role in epithelial cell apoptosis in bleomycin-induced fibrosis (35). Waghray and colleagues (36) demonstrated that UIP fibroblasts, when treated with transforming growth factor-β1, secreted H_2O_2 that induced apoptosis in bronchial epithelial cells cocultured with them. In this context, our finding of increased WNT5A in UIP lung fibroblasts, and the protective effects of WNT5A on normal lung fibroblasts from H_2O_2-induced apoptosis, may help to explain the fibroblasts part in this apoptosis paradox paradigm. WNT5A has been shown to prevent apoptosis also in uncommitted osteoblast progenitors and differentiated osteoblasts (37), dermal fibroblasts (38), and endothelial cells (39), supporting our results in primary lung fibroblasts.

Recently, there has been an interest in the role of the canonical β-catenin pathway in fibrosis (40). Our results suggest that, at least in primary lung fibroblasts, the noncanonical WNT/β-catenin pathway is also important, and that WNT5A exerts its effects through the noncanonical WNT/β-catenin pathway. WNT5A functions through several frizzled receptors on the cells surfaces (frizzled-2, -3, -4, -5, and -7) (41–44), as well as through the receptor tyrosine kinase-like orphan receptor 2 (45). WNT5A has been demonstrated to promote β-catenin degradation in cancer cells and in hematopoietic stem cells (46, 47). Furthermore, it has been observed that WNT5A partially inhibits apoptosis in dermal fibroblasts through inhibitory effect of cAMP-dependont protein kinase on GSK3β, which leads to β-catenin nucleation (38). Consistent with these results, we found that WNT5A caused decreases in β-catenin in all of the cell types that we examined (Figures 5A–5C). These decreases were neither associated with change in levels of total GSK3β (Figure 5K) or phosphorylation of GSK3β (ser 9) (Figure 5L), nor with phosphorylation of β-catenin at the serine 33, 37, or threonine 41 (Figure 5M) positions, as would be expected if WNT5A was active through the canonical WNT pathway. Instead, WNT5A induced an increase in the phosphorylation of β-catenin at the serine 45 and threonine 41(Figure 5N) positions, where it is phosphorylated by casein kinase 1α, suggesting an active role for WNT5A in promoting β-catenin degradation. Our results also provide further support to the results of Jiang and colleagues (48), who found no phosphorylation of β-catenin at the serine 33, 37, or threonine 41 positions, as well as no collection of β-catenin in nuclei of quiescent and activated rat hepatic stellate cells in response to WNT5A. Taken together with all of the above observations, our results suggest that β-catenin degradation in lung fibroblasts and A549 cells is regulated through the noncanonical WNT/β-catenin pathway. It is important to stress in this context that the WNT5A may have diverse effects that probably depend on cellular context. Although our results suggest that WNT5A may have a proproliferative and prosurvival effect on lung fibroblasts, Li and colleagues (49) demonstrated that mice constitutively lacking WNT5A expressed excessive lung cell proliferation, leading to interstitial condensation, but not affecting differentiation pattern of the epithelial and mesenchymal cells of mouse lungs. Their results suggest that, in the context of lung development, WNT5A may have an important role in limiting unregulated cellular proliferation, potentially through inhibiting β-catenin signaling. However, this effect of WNT5A may be context specific, and the functions of WNT5A may vary at different stages of organ development.

In this study, we focused on cells from human lung tissues. Unfortunately, there are no commercial recombinant human WNT5A proteins, so we used recombinant mouse WNT5A, as well as conditioned media of WNT5A-transfected mouse fibroblasts. We have observed the same effects of WNT5A in mouse lung fibroblasts and human lung fibroblasts (normal lung tissue, UIP) and A549 cells.

The starting point of this study was the comparison of gene expression patterns between fibroblasts from lung tissues with UIP histology and normal lung fibroblasts. We discovered that WNT5A gene expression was higher in UIP lung fibroblasts compared with normal lung fibroblasts. WNT5A significantly increased proliferation and inhibited apoptosis induced by H_2O_2 in normal lung fibroblasts; WNT5A inhibition caused an increase in active caspase-3. WNT5A also increased extracellular matrix production by elevating fibronectin and α5-integrin levels. Concomitantly, WNT5A caused a significant decrease in β-catenin levels that was not associated with changes in the canonical WNT/β-catenin signaling pathway. Our results suggest a role for WNT5A in regulating fibroblast proliferation and survival through the noncanonical WNT/β-catenin pathway, and thus suggest a role for this pathway in determining the lung phenotype in IPF and other progressive fibrotic interstitial lung diseases characterized by UIP histology.

Conflict of Interest Statement: N.K. is a recipient of investigator-initiated research grants from Biogen Idec ($674,800 in 2006) and from Centocor ($227,753 in 2007) for genomic and proteomic biomarker discovery and validation. Data presented in this article were not funded by any of these grants, nor are they related to the subject of these grants. None of the other authors has a financial relationship with a commercial entity that has an interest in the subject of this manuscript.

Acknowledgments: The authors thank Lara Chensny, Gouying Yu (Simmons Center), and Jason Devlin, Center of Biologic Imaging, University of Pittsburgh for their technical help.

References

1. Lynch J III, Saggar R, Weigt S, Zisman D, White E. Usual interstitial pneumonia. *Semin Respir Crit Care Med* 2006;27:634–651.
2. Katzenstein A, Myers J. Idiopathic pulmonary fibrosis: clinical relevance of pathologic classification. *Am J Respir Crit Care Med* 1998;157: 1301–1315.
3. Meltzer E, Noble P. Idiopathic pulmonary fibrosis. *Orphanet J Rare Dis* [serial on the Internet]. 2008;3:8. Available from: http://www.ojrd.com/content/3/1/8
4. Katzenstein A, Zisman D, Litzky L, Nguyen B, Kotloff R. Usual interstial pneumonia histologic study of biopsy and explant specimens. *Am J Surg Pathol* 2002;26:1567–1577.
5. Selman M, King TE Jr, Pardo A. Idiopathic pulmonary fibrosis: prevailing and evolving hypotheses about its pathogenesis and implications for therapy. *Ann Intern Med* 2001;134:136–151.
6. ATS/ERS International Multidisciplinary Consensus. Classification of the idiopathic interstitial pneumonias. *Am J Respir Crit Care Med* 2002;165:277–304.
7. Horowitz J, Thannickal V. Epithelial–mesenchymal interactions in pulmonary fibrosis. *Semin Respir Crit Care Med* 2006;27:600–612.
8. Flaherty K, Travis W, Colby T, Toews G, Kazerooni E, Gross B, Jain A, Strawderman R III, Flint A, Lynch J III, *et al.* Histopathologic variability in usual and nonspecific interstitial pneumonias. *Am J Respir Crit Care Med* 2001;164:1722–1727.
9. Selman M, Pardo A. Idiopathic pulmonary fibrosis: misunderstandings between epithelial cells and fibroblasts? *Sarcoidosis Vasc Diffuse Lung Dis* 2004;21:165–172.
10. Ward P, Hunninghake GW. Lung inflammation and fibrosis. *Am J Respir Crit Care Med* 1998;157:S123–S129.
11. Serini G, Gabbiani G. Mechanisms of myofibroblast activity and phenotypic modulation. *Exp Cell Res* 1999;250:273–283.
12. Selman M, Pardo A. Role of epithelial cells in idiopathic pulmonary fibrosis: from innocent targets to serial killers. *Proc Am Thorac Soc* 2006;3:364–372.
13. Raghu G, Chen Y, Rusch V, Rabinovitch PS. Differential proliferation of fibroblasts cultured from normal and fibrotic human lungs. *Am Rev Respir Dis* 1988;138:703–708.
14. Jordana M, Schulman J, McSharry C, Irving LB, Newhouse MT, Jordana G, Gauldie J. Heterogeneous proliferative characteristics of human adult lung fibroblast lines and clonally derived fibroblasts from control and fibrotic tissue. *Am Rev Respir Dis* 1988;137:579–584.
15. Pilewski JM, Liu L, Henry AC, Knauer AV, Feghali-Bostwick CA. Insulin-like growth factor binding protein 3 and 5 are overexpressed

in idiopathic pulmonary fibrosis and contribute to extracellular matrix deposition. *Am J Pathol* 2005;166:399–407.
16. Pierce EM, Carpenter K, Jakubzick C, Kunkel SL, Evanoff H, Flaherty KR, Martinez FJ, Toews GB, Hogaboam CM. Idiopathic pulmonary fibrosis fibroblasts migrate and proliferate to CC chemokine ligand 21. *Eur Respir J* 2007;29:1082–1093.
17. Pardo A, Selman M, Ramirez R, Ramos C, Montano M, Stricklin G, Raghu G. Production of collagenase and tissue inhibitor of metalloproteinases by fibroblasts derived from normal and fibrotic human lungs. *Chest* 1992;102:1085–1089.
18. Phan SH. The myofibroblast in pulmonary fibrosis. *Chest* 2002;122:286S–288S.
19. Zhang H, Gharaee-Kermani M, Zhang K, Phan SH. Lung fibroblast contractile and {alpha}-smooth muscle actin phenotypic alterations in bleomycin-induced pulmonary fibrosis. *Am J Pathol* 1996;148:527–537.
20. Desmouliere A, Gabbian G, Gabbian F, Geino A. Transforming growth factor-beta 1 induces alpha-smooth muscle actin expression in granulation tissue myofibroblasts and in quiescent and growing cultured fibroblasts. *J Cell Biol* 1993;122:103–111.
21. Hashimoto S, Gon Y, Takeshita I, Maruoka S, Horie T. IL-4 and IL-13 induce myofibroblastic phenotype of human lung fibroblasts through c-jun NH2-terminal kinase–dependent pathway. *J Allergy Clin Immunol* 2001;107:1001–1008.
22. Ramos C, Montaño M, García-Alvarez J, Ruiz V, Uhal B, Selman M, Pardo A. Fibroblasts from idiopathic pulmonary fibrosis and normal lungs differ in growth rate, apoptosis, and tissue inhibitor of metalloproteinases expression. *Am J Respir Cell Mol Biol* 2001;24:591–598.
23. Pardo A, Gibson K, Cisneros J, Richards T, Yang Y, Becerril C, Yousem S, Herrera I, Ruiz V, Selman M, *et al.* Up-regulation and profibrotic role of osteopontin in human idiopathic pulmonary fibrosis. *PLoS Med* 2005;2:e251.
24. Yang IV, Burch LH, Steele MP, Savov JD, Hollingsworth JW, McElvania-Tekippe E, Berman KG, Speer MC, Sporn TA, Brown KK, *et al.* Gene expression profiling of familial and sporadic interstitial pneumonia. *Am J Respir Crit Care Med* 2007;175:45–54.
25. Selman M, Carrillo G, Estrada A, Mejia M, Becerril C, Cisneros J, Gaxiola M, Perez-Padilla R, Navarro C, Richards T, *et al.* Accelerated variant of idiopathic pulmonary fibrosis: clinical behavior and gene expression pattern. *PLoS One* 2007;2:e482.
26. Selman M, Pardo A, Barrera L, Estrada A, Watson S, Wilson K, Aziz N, Kaminski N, Zlotnik A. Gene expression profiles distinguished idiopatic pulmonary fibrosis from hypersensitivity pneumonitis. *Am J Respir Crit Care Med* 2006;173:188–198.
27. Zuo F, Kaminski N, Eugui E, Allard J, Yakhini Z, Ben-Dor A, Lollini L, Morris D, Kim Y, Deustro B, *et al.* Gene expression analysis reveals matrilysin as a key regulator of pulmonary fibrosis in mice and humans. *Proc Natl Acad Sci USA* 2002;99:6292–6297.
28. Renzoni E, Abraham D, Howat S, Shi-Wen X, Sestini P, Bou-Gharios G, Wells A, Veeraraghavan S, Nicholson A, Denton C, *et al.* Gene expression profiling reveals novel TGFβ targets in adult lung fibroblasts. *Respir Res* 2004;5: 10.1186/1465–9921.
29. Novershtern N, Itzhaki Z, Manor O, Friedman N, Kaminsk N. A functional and regulatory map of asthma. *Am J Respir Cell Mol Biol* 2008;38:324–336.
30. Dave N, Kaminski N. Analysis of microarray experiments for pulmonary fibrosis. *Methods Mol Med* 2005;117:333–358.
31. Radom-Aizik S, Kaminski N, Hayek S, Halkin H, Cooper D, Ben-Dov I. Effects of exercise training on quadriceps muscle gene expression in chronic obstructive pulmonary disease. *J Appl Physiol* 2007;102:1976–1984.
32. Bouros D, Wells A, Nicholson A, Colby T, Polychronopoulos V, Pantelidis P, Haslam P, Vassilakis D, Black C, Du Bois R. Histopathologic subsets of fibrosing alveolitis in patients with systemic sclerosis and their relationship to outcome. *Am J Respir Crit Care Med* 2002;165:1581–1586.
33. Kuhn C, McDonald JA. The roles of the myofibroblast in idiopathic pulmonary fibrosis: ultrastructural and immunohistochemical features of sites of active extracellular matrix synthesis. *Am J Pathol* 1991;138: 1257–1265.
34. Thannickal VJ, Horowitz JC. Evolving concepts of apoptosis in idiopathic pulmonary fibrosis. *Proc Am Thorac Soc* 2006;3:350–356.
35. Wallach-Dayan S, Izbicki G, Cohen P, Gerstl-Golan R, Fine A, Breuer R. Bleomycin initiates apoptosis of lung epithelial cells by ROS but not by Fas/Fasl pathway. *Am J Physiol Lung Cell Mol Physiol* 2006; 290:790–796.
36. Waghray M, Cui Z, Horowitz JC, Sbramaniam IM, Martinez FJ, Toews GB, Thannickal VJ. Hydrogen peroxide is a diffusible paracrine signal for the induction of epithelial cell death by activated myofibroblasts. *FASEB J* 2005;19:854–856.
37. Almeida M, Han L, Bellido T, Manolagas SC, Kousteni S. Wnt proteins prevent apoptosis of both uncommitted osteoblast progenitors and differentiated osteoblasts by beta-catenin–dependent and –independent signaling cascades involving Src/ERK and phosphatidylinosito 3-kinase/AKT. *J Biol Chem* 2005;280:41342–41351.
38. Torii K, Nishizawa K, Kawasaki A, Yamashita Y, Katada M, Ito M, Nishimoto I, Terashita K, Aiso S, Matsuoka M. Anti-apoptotic action of WNT5A in dermal fibroblasts is mediated by the PKA signaling pathways. *Cell Signal* 2008;20:1256–1266.
39. Masckauchan NTH, Agalliu D, Vorontcikhina M, Ahn A, Parmalee NL, Li CM, Khoo A, Tycko B, Brown AMC, Kitajewski J. WNT5A signaling induces proliferation and survival of endothelial cells *in vitro* and expression of MMP-1 and TIE-2. *Mol Biol Cell* 2006;17:5163–5172.
40. Chilosi M, Poletti V, Zamo A, Lestani M, Montagna L, Piccoli P, Pedron S, Bertaso M, Scarpa A, Murer B, *et al.* Aberrant Wnt/beta-catenin pathway activation in idiopathic pulmonary fibrosis. *Am J Pathol* 2003;162:1495–1502.
41. Slusarski DC, Corces VG, Moon RT. Interaction of Wnt and a frizzled homologue triggers G-protein–linked phosphatidylinositol signalling. *Nature* 1997;390:410–413.
42. Chen W, Ten Bergge D, Brown J, Ahn S, Hu LA, Miller WE, Caron MG, Barak LS, Nusse R, Lefkowitz RJ. Dishevelled 2 recruits β-arrestin 2 to mediate WNT5A stimulated endocytosis of frizzled 4. *Science* 2003;301:1391–1394.
43. Sen M, Chamorro M, Reifert J, Corr M, Carson DA. Blockade of WNT5A/frizzled 5 signaling inhibits rheumatoid synoviocyte activation. *Arthritis Rheum* 2001;44:772–781.
44. Umbhauer M, Djiane A, Goisset C, Penzo-Mendez A, Riou J-F, Boucaut J-C, Shi D-L. The C-terminal cytoplasmic Lys-thr-X-X-X-Trp motif in frizzled receptors mediates Wnt/beta-catenin signalling. *EMBO J* 2000;19:4944–4954.
45. Mikels AJ, Nusse R. Purified WNT5A protein activates or inhibits beta catenin–TCF signaling depending on receptor context. *PLoS Biol* 2006;4:570–582.
46. Topol L, Jiang X, Choi H, Garrett-Beal L, Carolan PJ, Yang Y. WNT5A inhibits the canonical wnt pathway by promoting GSK-3–independent β-catenin degradation. *J Cell Biol* 2003;162:899–908.
47. Nemeth M, Topol L, Anderson S, Yang Y, Bodine D. WNT5A inhibits canonical Wnt signaling in hematopoietic stem cells and enhances repopulation. *Proc Natl Acad Sci USA* 2007;104:15436–15441.
48. Jiang F, Parsons CJ, Stefanovic B. Gene expression profile of quiencent and activated rat hepatic stellate cells implicates Wnt signaling pathway action. *J Hepatol* 2006;45:401–409.
49. Li C, Xiao J, Hormi K, Borok Z, Minoo P. Wnt5A participates in distal lung morphogenesis. *Dev Biol* 2002;248:68–81.